Relativistic precession and spin dynamics of an elliptic Rydberg wave packet

2002 J. Phys. A: Math. Gen. 35 7803

(http://iopscience.iop.org/0305-4470/35/36/308)

INSTITUTE OF PHYSICS PUBLISHING JOURNAL OF PHYSICS A: MATHEMATICAL AND GENERAL

J. Phys. A: Math. Gen. **35** (2002) 7803–7816 PII: S0305-4470(02)32802-6

Relativistic precession and spin dynamics of an elliptic Rydberg wave packet

P Rozmej[1], **M Turek**[2], **R Arvieu**[3] **and I S Averbukh**[4]

[1] Institute of Physics, University of Zielona Góra, 65-246 Zielona Góra, Poland
[2] Institute of Physics, Maria Curie-Skłodowska University, 20-031 Lublin, Poland
[3] Institut des Sciences Nucléaires, F 38026 Grenoble Cedex, France
[4] The Weizmann Institute of Science, 76100 Rehovot, Israel

E-mail: p.rozmej@im.pz.zgora.pl, mturek@kft.umcs.lublin.pl, arvieu@in2p3.fr and ilya.averbukh@weizmann.ac.il

Received 17 January 2002
Published 28 August 2002
Online at stacks.iop.org/JPhysA/35/7803

Abstract

The time evolution of wave packets (WPs) built from the eigenstates of the Dirac equation for a hydrogenic system is considered. We investigate the space and spin motion of wave packets which, in the non-relativistic limit, are stationary states with a probability density distributed almost uniformly along the classical, elliptical orbit (elliptic WP). We show that the precession of such a WP, due to relativistic corrections to the energy eigenvalues, is strongly correlated with the spin motion. We also show that the motion is universal for all hydrogenic systems with an arbitrary value of the atomic number Z.

PACS numbers: 03.65.P, 03.65, 03.65.S

The detailed study of the time evolution of quantum wave packets (WPs) in simple atomic or molecular systems has been the object of growing attention for more than ten years [1]. Most of the previous theoretical studies were done in a non-relativistic framework. In the field of relativistic quantum mechanics most of the efforts have been focused on the problem of the interaction between the atoms and a mixture of static fields with, most of the time, intense laser fields [2–11]. Under these conditions the use of a relativistic theory is fully justified since the external field is then able to bring considerable energy to the WP. For isolated atoms, however, the use of relativistic dynamics is more questionable if the WP is followed or observed only for a short period of time. In [12] relativistic wave packets, corresponding to circular orbits, have been constructed for hydrogenic atoms with a large Z, and propagated over time according to the Dirac equation. Particular attention was paid to the spin collapse event, i.e. to the maximum entanglement, in the course of time, of the spin degree of freedom with the spatial ones. This phenomenon was first shown to take place for a WP in a harmonic oscillator with a spin–orbit force [13], where it is periodic. For this reason it has been called the *spin–orbit pendulum*. In the Dirac equation with a Coulomb potential, it is produced by the built-in

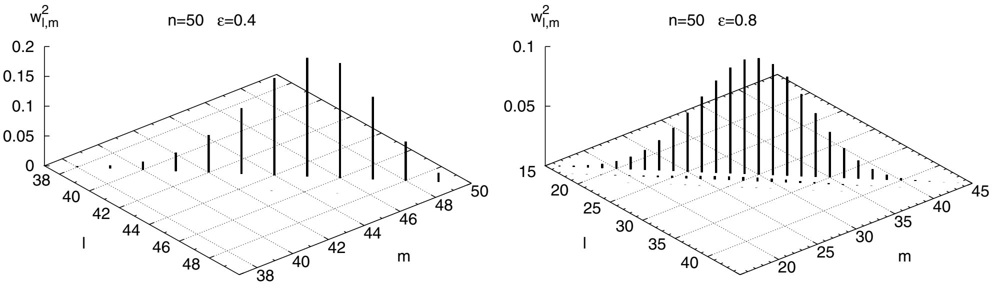

Figure 1. Squares of coefficients of the expansion (1) for $n = 50, \epsilon = 0.4$ (left) and $\epsilon = 0.8$ (right).

spin–orbit interaction and is not periodic. The timescale where this effect can manifest itself was discussed in [12], as a function of the charge Z of the atom and the average principal quantum number n of the WP. This phenomenon is expected to take place on a longer timescale similar to the other time-dependent quantum effects of spreading and fractional revivals [14]. We intend below to complement this work by studying the possible relativistic precession of elliptic WPs and by comparing this precession to the spin motion. A preliminary version of the present work was already presented at the ECAMP VII conference [15].

There are two possible ways to build up a WP 'on top of a classical elliptic orbit' in non-relativistic mechanics. One of them is by kicking a well-designed WP properly, for example a Gaussian WP, that is then evolved in time by the free Hamiltonian until it spreads above an average classical ellipse. This method is not very easy to apply and its main inconvenience is to produce an internal motion within the ellipse that is able to blur the precession. Therefore, we have preferred a second, much simpler method that consists of using the coherent WPs of [16], which are stationary states of the non-relativistic Coulomb problem. The space probability density of these states was indeed shown to be highly concentrated around a classical Bohr–Sommerfeld ellipse. If these states can be adapted to relativistic dynamics their time evolution will doubtlessly be due to relativistic effects, i.e. due to the fine structure that will act as a perturbation. Let us first show how to adapt these states to a relativistic theory. We want the spatial part of the large components of the new WP to tend (in the non-relativistic limit) towards the state $|n\gamma\rangle$ of [16] which is defined as

$$|n\gamma\rangle = \sum_{l,m} (-1)^{(l+m)/2} \frac{2^{n-l-1}(n-1)!}{[(l-m)/2]![(l+m)/2]!} \left[\frac{(l+m)!(l-m)!(2l+1)}{(n-l-1)!(n+l)!}\right]^{1/2} \times \left(\sin\frac{\gamma}{2}\right)^{n-m-1} \left(\cos\frac{\gamma}{2}\right)^{n+m-1} |n,l,m\rangle = \sum_{lm} w^{(n)}_{lm} |n,l,m\rangle. \tag{1}$$

The probability density $\langle n\gamma|n\gamma\rangle$ is fairly localized onto a Bohr orbit with eccentricity $\epsilon = \sin\gamma$ and the average angular momentum is

$$l_{av} = (n-1)\cos\gamma \tag{2}$$

where n is the principal quantum number of the orbitals $|n,l,m\rangle$ which are admixed in (1). The sum contains $n(n+1)/2$ values of m with even $l+m$. The contribution of states with $m < l$ decreases very rapidly with m (more than one order of magnitude for each two units of m as shown in figure 1). The dominant weights are those with $m = l$ and their distribution is nearly Gaussian. The relative contribution of states with $m < l$ increases, however, for larger values of the eccentricity parameter ϵ. The larger admixture of these states causes much faster

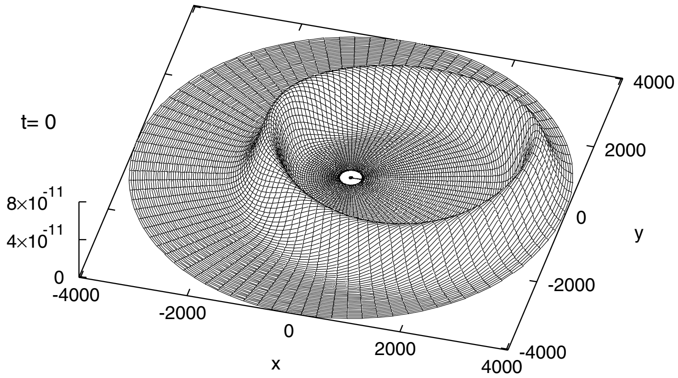

Figure 2. The initial probability density of the relativistic WP (5) with $n = 50$, $\epsilon = 0.4$ and $Z = 92$ in the plane of the classical orbit. The distance is given in units a_0/Z, where $a_0 \approx 5.29 \times 10^{-11}$ m is the Bohr radius. See further discussion on Z dependence.

dephasing of the WP. Therefore, for illustration of typical precession phenomena we have chosen the case $\epsilon = 0.4$.

In order to study the entanglement of the spin degrees of freedom with the orbital ones, it is natural in a non-relativistic theory to start from a product state of an arbitrary spinor $\binom{a}{b}$ with the state $|n\gamma\rangle$.

$$|\Psi_{nr}\rangle = |n\gamma\rangle \begin{pmatrix} a \\ b \end{pmatrix} = \sum_{lm} w_{lm}^{(n)} |n, l, m\rangle \begin{pmatrix} a \\ b \end{pmatrix}. \tag{3}$$

It may be expanded in eigenstates of total angular momentum $|n, l, j = l + s, m_j\rangle$ with $m_j = m + 1/2$ or $m - 1/2$ and $s = +1/2$ or $-1/2$

$$|\Psi_{nr}\rangle = \sum_{lm} w_{lm}^{(n)} \left\{ a \left(\sqrt{\frac{l+1+m}{2l+1}} |n, l, j_>, m + 1/2\rangle - \sqrt{\frac{l-m}{2l+1}} |n, l, j_<, m + 1/2\rangle \right) \right.$$
$$\left. + b \left(\sqrt{\frac{l+1-m}{2l+1}} |n, l, j_>, m - 1/2\rangle + \sqrt{\frac{l+m}{2l+1}} |n, l, j_<, m - 1/2\rangle \right) \right\}. \tag{4}$$

In a similar way as in [12], for a circular WP, the state (4) is transformed into a four component relativistic state Ψ_r by replacing in (4) the non-relativistic states $|n, l, j, m_j\rangle$ by the eigenstates of the Dirac equation with the same quantum numbers. In this manner the WP gets small components in the most natural way. The radial parts of the large and of the small components are taken obviously as different ones. The probability density of the relativistic WP built in this way is represented in figure 2.

The time evolution of the WP is produced by introducing the phase factors $\exp\left(-\mathrm{i}E_l^+ t\right)$ and $\exp\left(-\mathrm{i}E_l^- t\right)$ as coefficients of states with $j = l + 1/2$ and $j = l - 1/2$ with their corresponding eigenvalues. The four components $c_i(t)$ $i = 1, \ldots, 4$ of the WP at time t are given in appendix A with Ψ_r defined as

$$|\Psi_r(t)\rangle = \begin{pmatrix} |c_1(t)\rangle \\ |c_2(t)\rangle \\ |c_3(t)\rangle \\ |c_4(t)\rangle \end{pmatrix}. \tag{5}$$

It should be stressed that for $t = 0$ Ψ_r is no longer a product state of the form of equation (3) due to the built-in entanglement contained in the solutions of the Dirac equation. However, since the small components of Ψ_r are indeed very small, this defect has no important effect on the magnitude of the initial spin. Since the spin–orbit coupling effect, i.e. spin–orbit pendulum [13], manifests itself more efficiently if s and l are perpendicular to each other, we choose for our discussion:

$$a = b = \frac{1}{\sqrt{2}} \qquad \text{i.e.} \qquad \langle s_x \rangle_{nr} = \frac{1}{2}. \tag{6}$$

Precession of quantum elliptical states in the Coulomb field has already been considered in [17], starting also from the same coherent state as given here. However, the precession was studied only in non-relativistic quantum dynamics as a perturbation effect and no treatment of the spin was attempted.

Let us finally discuss the time units relevant to our problem. To the lowest order in terms of the fine structure constant, the energy of an eigenstate $|n, l, j = l + s\rangle$ of the Dirac equation can be written (in au) for a hydrogenic atom of charge Z as

$$E_{nlj} = \overline{E}_n - \frac{1}{2}\frac{Z^4\alpha^2}{n^3(l+s+1/2)} \tag{7}$$

with $s = +1/2$ or $-1/2$. The constant energy $\overline{E}_n$ produces no effect on WP, since it depends only on n. Let us define an average time unit T_p (p for precession):

$$T_p = \frac{2\pi}{\left\langle \frac{\mathrm{d}E_{nlj}}{\mathrm{d}l} \right\rangle} \tag{8}$$

$$= \frac{4\pi n^3}{Z^4\alpha^2}\left\langle \left(l + s + \frac{1}{2}\right)^2 \right\rangle \approx \frac{4\pi n^3 l_{av}^2}{Z^4\alpha^2} \tag{9}$$

$$= \frac{2 l_{av}^2 T_K}{(Z\alpha)^2}. \tag{10}$$

Brackets $\langle\rangle$ in (8) and (9) denote average values, l_{av} is given by (2). For $n = 50, \epsilon = 0.4$ precession time T_p ranges from 1.96×10^{-11} s for $Z = 92$ to 1.4×10^{-3} s for $Z = 1$. T_K in (10) denotes the Kepler period.

It is necessary to compare T_p to the radiative lifetime $T_{n,l}^{\mathrm{rad}}$ of hydrogenic levels. We will use the estimation of $T_{n,l}^{\mathrm{rad}}$ for a single n, l state given in [18]. In atomic units it is

$$T_{n,l}^{\mathrm{rad}} = \frac{3}{2\alpha^3 Z^4} n^3 \left(l + \frac{1}{2}\right)^2 \tag{11}$$

which was found to agree within 10% with experimental data. One obtains the universal ratio:

$$\frac{T_p}{T_{n,l}^{\mathrm{rad}}} = \frac{8\pi\alpha}{3} \approx 0.061 \tag{12}$$

which guarantees that the precession of the wave packet takes place long enough before even a single photon is emitted. The occurrence of α in this ratio is understandable, since T_p is a classical-like quantity, while $T_{n,l}^{\mathrm{rad}}$ is proportional to $\hbar$, because it can be expressed as the ratio of a typical energy of the emitted photon to the classical radiation rate corresponding to the orbital motion.

When $t = T_p$ the linear terms in the expansion of E_{nlj} in the power of l give a contribution of 2π in the exponential factors, leading to a restoration of the WP. However, the terms of higher order dephase the various partial waves differently, and this leads to a spreading of the WP near the initial shape [14] (see the discussion on the magnitude of these terms in appendix B). Expression (9) or (10) (with the Kepler period $T_K = 2\pi n^3/Z^2$) is also recognized as the classical precession time in the relativistic Coulomb problem [19].

We note that $\mathrm{d}E_{nlj}/\mathrm{d}l$ is also (to the first order) the energy difference between the two spin–orbit partners. Therefore the precession time can also be interpreted as the recurrence time of the spin. Hence we should observe a strong correlation between the spatial motion of the density, the precession, and the spin motion.

We now discuss the dynamics dependence on the atomic number, Z. Formula (9) suggests that the relativistic effects under consideration in this paper depend crucially on Z. The highest possible Z is indeed required to lower T_p as much as possible. It is interesting to stress, nevertheless, that within a very good approximation, a scaling of Z is possible which leads to the universal behaviour of the wave packet (1).

First of all since E, approximated by equation (7), scales as Z^4, i.e. as T_p^{-1}, the variable Z disappears from Et if we use the reduced time t/T_p. The autocorrelation function (A.20) which is expressed only in terms of Et is the simplest quantity which has a universal behaviour, provided the same n and ϵ are used for all values of Z.

The other quantities, such as the probability density and the spin expectation values, depend on the radial wavefunctions and radial integrals. In a non-relativistic theory scaling of the radial wavefunction is elementary, it is obtained by dividing the radial wavefunction by $Z^{3/2}$ and multiplying the radial variable by Z. This is an exact property. The ratio of small/large components of the relativistic solutions scales as $\sqrt{(1-E)/(1+E)}$, i.e. roughly as Z^2 and the radial wavefunctions also depend on Z in a more complicated manner. Nevertheless, on the whole, as seen in figure 5 below, the small components contribute a very small part of the probability density even for $Z = 92$ (see also figure 1 of [12]). The scaling of the probability density is therefore entirely governed by the large components, i.e. by the non-relativistic theory.

In a similar way we have checked that the radial integrals which contribute to the spin expectation values have the same properties: the integrals G_+, G_- and G_{+-} are equal to 1, within less than 10^{-5} and the other F_+, F_-, ... contribute in a very small manner, also of the order of 10^{-5}.

Therefore, the universal behaviour of the wave packet is justified and except for figure 2 no value of Z is given. For longer times, the energy factors omitted in equation (7) which involve higher powers of Z, play a role and produce a genuine Z dependence. Those effects will not be discussed here.

The probability density of the wave packet with $n = 50$, $\epsilon = 0.4$ and $a = b = 1/\sqrt{2}$, with $Z = 92$, is shown for a set of times up to $t = T_p$ in figures 3 and 4. The part of the density coming from the small components, shown in figure 5, is also concentrated on top of an ellipse but its magnitude is a thousand times smaller than the total density. For $t < T_p/4$ the density precesses as described classically with a small dispersion. However, the spreading takes place very rapidly for larger t and is quite extended for $t = T_p$.

The precession of the ellipse, the recurrence and spreading can be seen in a more condensed manner in the autocorrelation function represented in figure 6 for three different spin preparations (spin up, spin down and $a = b = 1/\sqrt{2}$). For small t/T_p the WP becomes almost orthogonal to its initial parent, for $t = T_p$ a recurrence occurs but the overlap is only 0.7. Another peak occurs at $t = 2T_p$ but higher frequencies become important and spread the recurrence. For $t > 3T_p$ these higher frequencies play a dominant role. An example of an approximate revival for $t = 22.6T_p$ is displayed in figure 7. Fractional revivals [14] can also be seen to some extent. Two examples of 1/3 and 1/2 revivals are presented in figure 8.

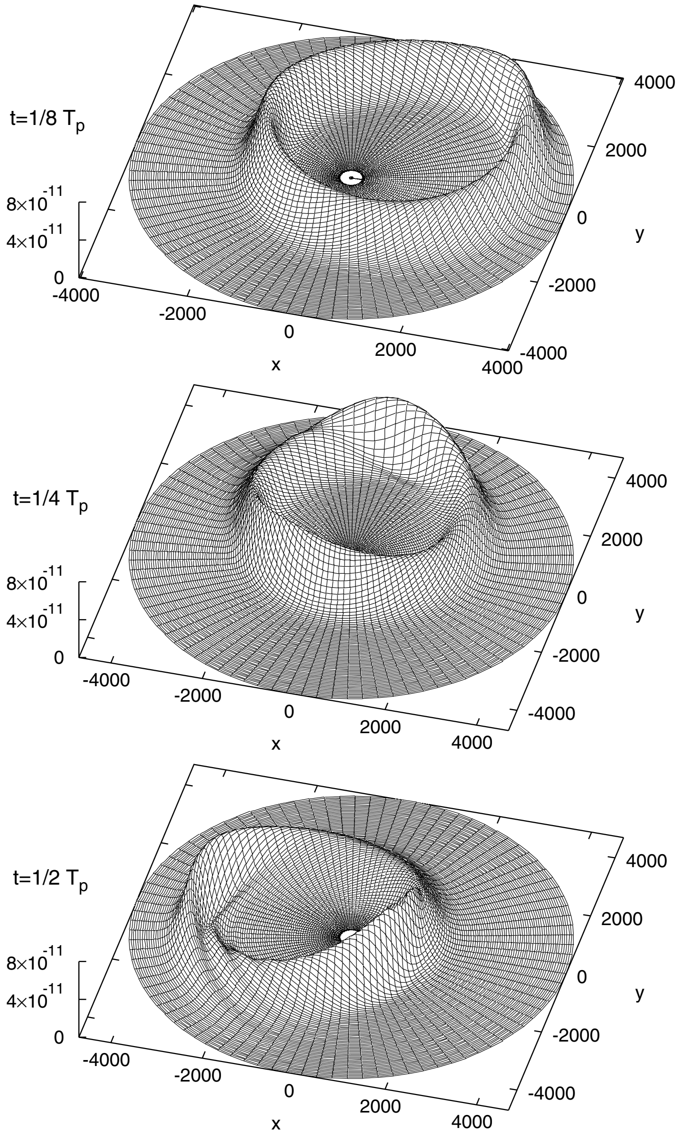

Figure 3. The probability density of the relativistic WP (5) on the plane of the classical orbit, during the first half of the precession period.

The rough independence of the autocorrelation function from the spin preparation requires some explanation. We can approximate this function by

$$\langle \Psi_r(0)|\Psi_r(t)\rangle \approx a^2 \sum_l w_{ll}^2 \exp\left(-\mathrm{i}E_l^+ t\right) + b^2 \sum_l w_{ll}^2 \exp\left(-\mathrm{i}E_l^- t\right) \tag{13}$$

where we have neglected the terms with very small weights $w_{l,m\neq l}^2$. The contribution of the two sums above is almost the same because w_{ll} has a smooth variation with l on the one hand, and because of the exact equality $E_l^- = E_{l-1}^+$ on the other hand. Finally, the time evolution of the spin average is presented in figure 9. This figure exhibits what we can call the relativistic spin–orbit pendulum. Although the wave packet is not prepared initially in a

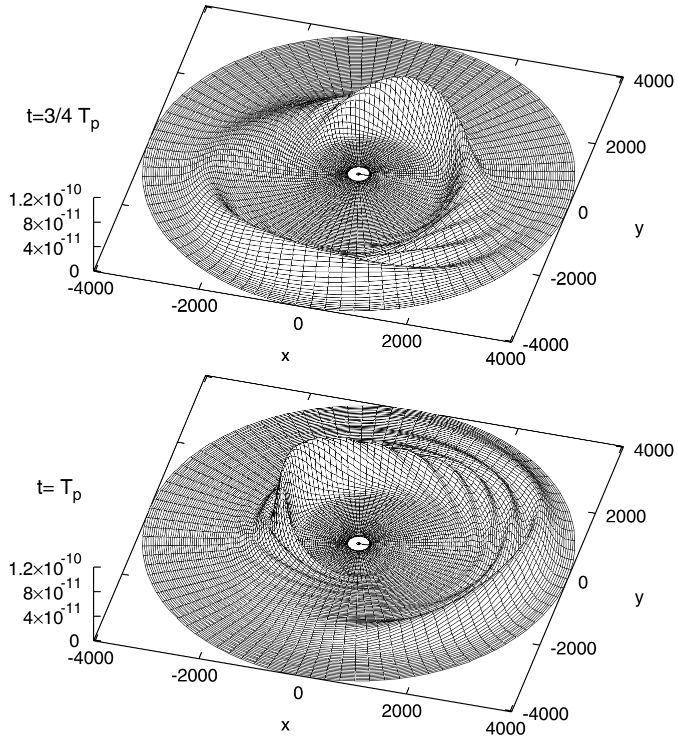

Figure 4. The same as in figure 3, but during later stages of the first period of precession.

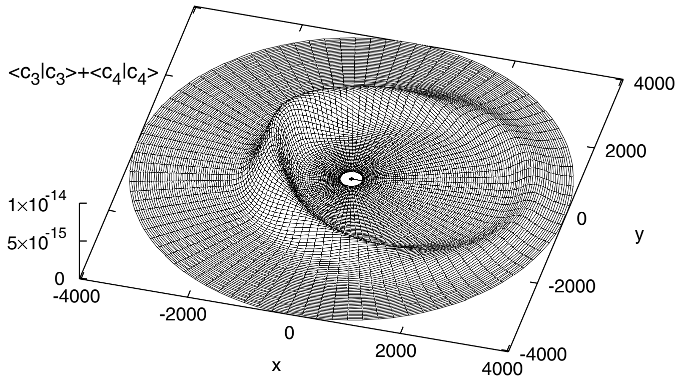

Figure 5. The contribution of the small components to the initial probability density. Note that the vertical scale is a thousand times smaller than that in the previous figures.

pure state of spin, the impurity is very small (for $a = b = 1/\sqrt{2}$ one has $\langle\sigma_x\rangle \approx 0.9997$). As time goes on the spin stays very nearly in the Oxy plane and rotates around Oz with period T_p. Its magnitude slowly decreases, however, and for $5 < t/T_p < 10$ the spin is almost totally entangled with the orbital motion, since the average of its three projections is almost zero. During a period of time that lasts for about $5T_p$ the angular momentum of the spin is transferred to the orbital motion and therefore the mean trajectory is not planar anymore [13]. Since the orbital angular momentum of $40\hbar$ is much higher than $\hbar/2$ this geometrical

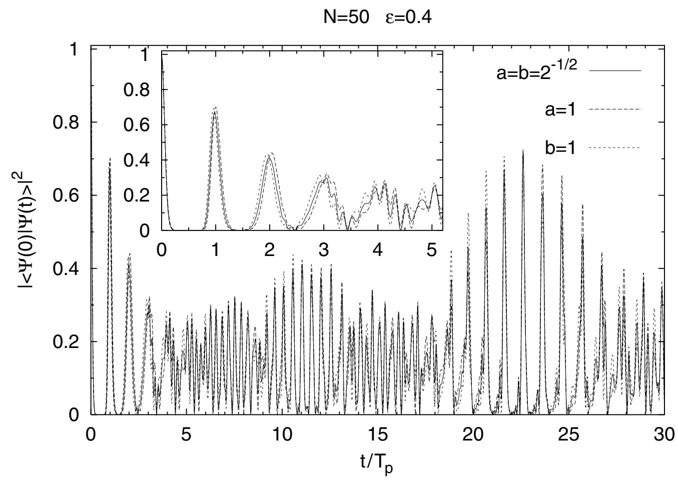

Figure 6. The autocorrelation function for three different spin preparations. The short time dependence is presented in the inset.

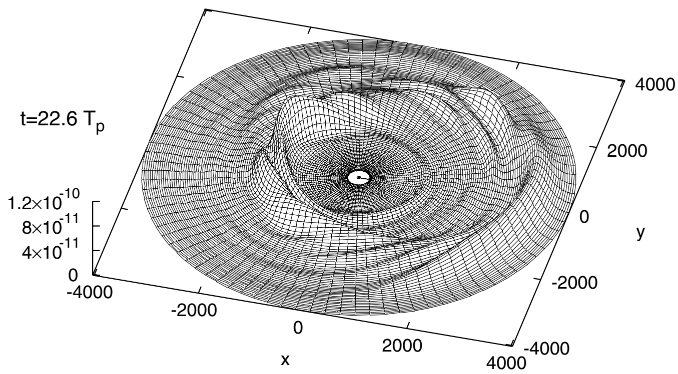

Figure 7. Example of the approximate revival of the elliptic wave packet. The value of recurrence probability is 0.73.

effect can hardly be represented graphically. From $t \approx 15T_p$ a revival of spin occurs. The spin rotates and increases its magnitude at the same time. This event stays even longer than initially. However, the recurrence is only partial.

In conclusion we can say that for not too long time, the precession and spin motion of the WPs are fairly well described by the following approximation: non-relativistic wavefunctions of the form (3) and relativistic energy eigenvalues. From this point of view the full, computationally very demanding, relativistic approach is unnecessary. However, this conclusion may be formulated not *a priori* but only *a posteriori*.

We would like to stress the richness of the dynamics just described. Indeed, in addition to the relativistic precession of the ellipse we have found its fractional revivals at longer times. During the evolution the spin of the electron is entangled with its orbital motion to various degrees. All this agrees completely with previous results [13, 14]. However, it was obtained here in a full relativistic calculation. Since we have been able to scale the atomic number Z we have given a universal behaviour to our WP. It is, however, clear that this scaling is destroyed

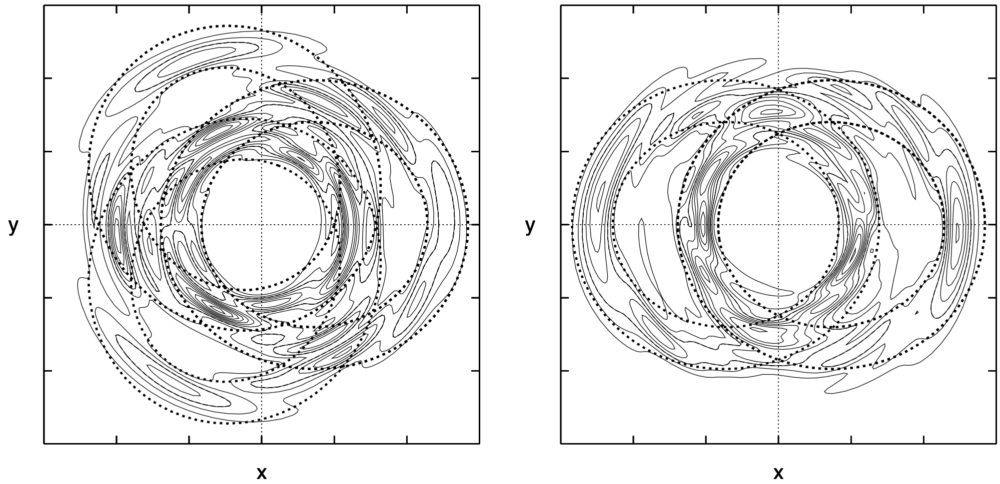

Figure 8. Examples of the approximate $1/3$ revival (left, $t = 7.525T_p$) and $1/2$ revival (right, $t = 11.045T_p$) of the elliptic wave packet as contour plots. The thick lines mark the shape of the initial probability density rotated by an appropriate angle.

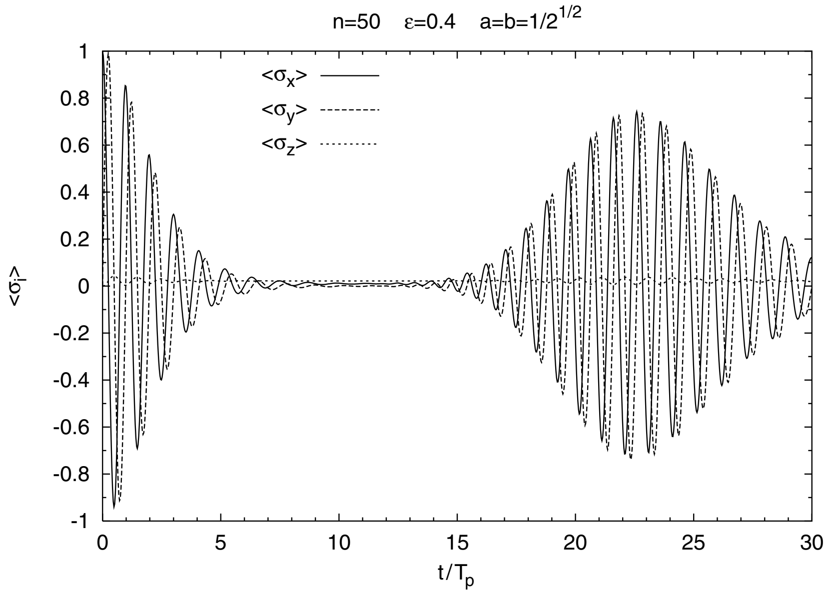

Figure 9. Time evolution of expectation values of spin components.

in real atoms in a more realistic theory which would take into account quantum defects. Their inclusion would also distort the dynamics, for example it would change the precession time, in a way that is out of the reach of our simple theory. As far as purely relativistic effects are concerned, such as the importance of the small components or the zitterbewegung, we have found them to be negligible in the Coulomb problem, in contrast to the Dirac oscillator [20] in which they play a major role.

Acknowledgments

The authors would like to express their gratitude to the two referees who attracted the authors' attention to the interplay between relativistic precession and radiative processes (equation (12)) in the Coulomb problem. I S Averbukh also thanks C R Stroud, Jr. for useful discussions.

This research was supported in part by Polish KBN through Grants no 5 P03B 010 20 and 5 P03B 104 21.

Appendix A. Details of the calculations

Replacing a non-relativistic wavefunction in (4) by the eigenstates of the Dirac equation, one obtains for $\Psi_r(t)$

$$\Psi_r(t) = \sum_{lm} w_{lm}^{(n)} \left\{ a\sqrt{\frac{l+1+m}{2l+1}} \begin{pmatrix} \mathrm{i}g_{n'_+}\Omega_{l,j_>,m+1/2} \\ -f_{n'_+}\Omega_{l+1,j_>,m+1/2} \end{pmatrix} \exp\left(-\mathrm{i}E_l^+ t\right) \right.$$
$$+ a\sqrt{\frac{l-m}{2l+1}} \begin{pmatrix} \mathrm{i}g_{n'_-}\Omega_{l,j_<,m+1/2} \\ -f_{n'_-}\Omega_{l-1,j_<,m+1/2} \end{pmatrix} \exp\left(-\mathrm{i}E_l^- t\right)$$
$$+ b\sqrt{\frac{l+1-m}{2l+1}} \begin{pmatrix} \mathrm{i}g_{n'_+}\Omega_{l,j_>,m-1/2} \\ -f_{n'_+}\Omega_{l+1,j_>,m-1/2} \end{pmatrix} \exp\left(-\mathrm{i}E_l^+ t\right)$$
$$\left. - b\sqrt{\frac{l+m}{2l+1}} \begin{pmatrix} \mathrm{i}g_{n'_-}\Omega_{l,j_<,m-1/2} \\ -f_{n'_-}\Omega_{l-1,j_<,m-1/2} \end{pmatrix} \exp\left(-\mathrm{i}E_l^- t\right) \right\}. \tag{A.1}$$

We have used the notation of [12]: $g(r)$ and $f(r)$ are the radial parts of the large and small components associated with the quantum numbers $n' = n - (j + 1/2)$. These functions are multiplied by the spherical tensors Ω_{l,j,m_j} which are defined by equations (4*a*) and (4*b*) of [12]. The energy of the spin–orbit partners of a given value of l is denoted by E_l^+ if $j = l + 1/2$ and E_l^- if $j = l - 1/2$, respectively.

For numerical calculations it is convenient to rewrite components of (A.1) in the following form:

$$|c_1(t)\rangle = \mathrm{i}\sum_l \left\{ g_{n'_+} \exp\left(-\mathrm{i}E_l^+ t\right) \sum_m w_{lm}^{(n)} \left(a\frac{l+1+m}{2l+1}|l,m\rangle \right.\right.$$
$$\left. + b\frac{\sqrt{(l+1-m)(l+m)}}{2l+1}|l,m-1\rangle \right)$$
$$+ g_{n'_-} \exp\left(-\mathrm{i}E_l^- t\right) \sum_m w_{lm}^{(n)} \left(a\frac{l-m}{2l+1}|l,m\rangle \right.$$
$$\left.\left. - b\frac{\sqrt{(l+1-m)(l+m)}}{2l+1}|l,m-1\rangle \right) \right\} \tag{A.2}$$

$$|c_2(t)\rangle = \mathrm{i}\sum_l \left\{ g_{n'_+} \exp\left(-\mathrm{i}E_l^+ t\right) \sum_m w_{lm}^{(n)} \left(b\frac{l+1-m}{2l+1}|l,m\rangle \right.\right.$$
$$\left. + a\frac{\sqrt{(l+1+m)(l-m)}}{2l+1}|l,m+1\rangle \right)$$
$$+ g_{n'_-} \exp\left(-\mathrm{i}E_l^- t\right) \sum_m w_{lm}^{(n)} \left(b\frac{l+m}{2l+1}|l,m\rangle \right.$$
$$\left.\left. - a\frac{\sqrt{(l+1+m)(l-m)}}{2l+1}|l,m+1\rangle \right) \right\} \tag{A.3}$$

$$
\begin{aligned}
|c_3(t)\rangle = \sum_l \Bigg\{ & f_{n'_+} \exp\left(-\mathrm{i}E_l^+ t\right) \sum_m w_{lm}^{(n)} \left(a\sqrt{\frac{(l+1+m)(l+1-m)}{(2l+1)(2l+3)}} |l+1, m\rangle \right. \\
& \left. + b\sqrt{\frac{(l+1-m)(l+2-m)}{(2l+1)(2l+3)}} |l+1, m-1\rangle \right) \\
& + f_{n'_-} \exp\left(-\mathrm{i}E_l^- t\right) \sum_m w_{lm}^{(n)} \left(a\sqrt{\frac{(l+m)(l-m)}{(2l+1)(2l-1)}} |l-1, m\rangle \right. \\
& \left. - b\sqrt{\frac{(l+m)(l-1+m)}{(2l+1)(2l-1)}} |l-1, m-1\rangle \right) \Bigg\}
\end{aligned} \tag{A.4}
$$

$$
\begin{aligned}
|c_4(t)\rangle = \sum_l \Bigg\{ & f_{n'_+} \exp\left(-\mathrm{i}E_l^+ t\right) \sum_m w_{lm}^{(n)} \left(-b\sqrt{\frac{(l+1+m)(l+1-m)}{(2l+1)(2l+3)}} |l+1, m\rangle \right. \\
& \left. - a\sqrt{\frac{(l+1+m)(l+2+m)}{(2l+1)(2l+3)}} |l+1, m+1\rangle \right) \\
& + f_{n'_-} \exp\left(-\mathrm{i}E_l^- t\right) \sum_m w_{lm}^{(n)} \left(-b\sqrt{\frac{(l+m)(l-m)}{(2l+1)(2l-1)}} |l-1, m\rangle \right. \\
& \left. + a\sqrt{\frac{(l-m)(l-1-m)}{(2l+1)(2l-1)}} |l-1, m+1\rangle \right) \Bigg\}.
\end{aligned} \tag{A.5}
$$

Using the explicit form of the WP, one obtains for the average values of the spin operators

$$
\begin{aligned}
\langle \sigma_x \rangle_t = 2ab \sum_{lm} \Bigg\{ & w_{l,m}^2 \left[G_+ \frac{(l+1)^2 - m^2}{(2l+1)^2} + G_- \frac{l^2 - m^2}{(2l+1)^2} - F_+ \frac{(l+1)^2 - m^2}{(2l+1)(2l+3)} \right. \\
& \left. - F_- \frac{l^2 - m^2}{(2l+1)(2l-1)} + 2G_{+-} \frac{l(l+1) + m^2}{(2l+1)^2} \cos(\omega_l t) \right] + w_{l,m} w_{l-2,m-2} \\
& \times \left[F_{-+} \sqrt{\frac{(l+m)(l-1+m)(l-2+m)(l-3+m)}{(2l-1)^2(2l+1)(2l+3)}} \cos(\omega_l'' t) \right] \\
& + w_{l,m} w_{l,m-2} \frac{\sqrt{(l+m)(l-1+m)}}{(2l+1)} \left[\frac{\sqrt{(l+1-m)(l+2-m)}}{(2l+1)} \right. \\
& \times [G_+ + G_- - 2G_{-+} \cos(\omega_l t)] - \frac{\sqrt{(l+2-m)(l-3-m)}}{(2l-1)} F_- \\
& \left. - \frac{\sqrt{(l+2-m)(l+1-m)}}{(2l+3)} F_+ \right] - w_{l,m} w_{l-2,m} \\
& \times \left[2F_{-+} \sqrt{\frac{(l^2 - m^2)((l-1)^2 - m^2)}{(2l-1)^2(2l+1)(2l-3)}} \cos(\omega_l'' t) \right] + w_{l,m} w_{l+2,m-2} \\
& \times \left[F'_{-+} \sqrt{\frac{(l+1-m)(l+2-m)(l+3-m)(l+4-m)}{(2l+1)(2l+3)^2(2l+5)}} \cos(\omega_l' t) \right] \Bigg\}
\end{aligned} \tag{A.6}
$$

$$\langle\sigma_y\rangle_t = 2ab\sum_{lm}\left\{w_{l,m}^2\left[\frac{2m}{2l+1}G_{+-}\sin(\omega_l t)\right]\right.$$
$$-\,w_{l,m}w_{l-2,m-2}\left[F_{-+}\sqrt{\frac{(l+m)(l-1+m)(l-2+m)(l-3+m)}{(2l-1)^2(2l+1)(2l+3)}}\sin(\omega_l'' t)\right]$$
$$+\,w_{l,m}w_{l-2,m}\left[2F_{-+}\sqrt{\frac{(l^2-m^2)((l-1)^2-m^2)}{(2l-1)^2(2l+1)(2l-3)}}\sin(\omega_l'' t)\right]-w_{l,m}w_{l+2,m-2}$$
$$\left.\times\left[F_{-+}'\sqrt{\frac{(l+1+m)(l+2-m)(l+3-m)(l+4-m)}{(2l-1)(2l+3)^2(2l+5)}}\sin(\omega_l' t)\right]\right\} \tag{A.7}$$

and

$$\langle\sigma_z\rangle_t = \sum_{lm}\left\{w_{l,m}^2\left[a^2\frac{2m+1}{2l+1}\left(G_+\frac{l+1+m}{2l+1}-G_-\frac{l-m}{2l+1}-F_+\frac{l+1+m}{2l+3}+F_-\frac{l-m}{2l-1}\right)\right.\right.$$
$$+\,b^2\frac{2m-1}{2l+1}\left(G_+\frac{l+1-m}{2l+1}-G_-\frac{l+m}{2l+1}-F_+\frac{l+1-m}{2l+3}+F_-\frac{l+m}{2l-1}\right)$$
$$\left.+\,4G_{+-}\cos(\omega_l t)\left(a^2\frac{(l-m)(l+1+m)}{(2l+1)^2}-b^2\frac{(l+m)(l+1-m)}{(2l+1)^2}\right)\right]$$
$$\left.+\,4(a^2-b^2)w_{l,m}w_{l+2,m}F_{-+}'\sqrt{\frac{((l+1)^2-m^2)((l+2)^2-m^2)}{(2l+1)(2l+3)^2(2l+5)}}\cos(\omega_l' t)\right\}. \tag{A.8}$$

In the above formulae, the following notation has been introduced:

$$\omega_l = \left(E_l^+ - E_l^-\right) \tag{A.9}$$

$$\omega_l' = \left(E_{l+2}^- - E_l^+\right) \tag{A.10}$$

$$\omega_l'' = \left(E_l^- - E_{l-2}^+\right). \tag{A.11}$$

Note that $\omega_l' = \omega_{l+2}''$. Radial integrals are denoted as follows:

$$G_+ = \int_0^\infty \left(g_l^+(r)\right)^2 r^2\,\mathrm{d}r \tag{A.12}$$

$$G_- = \int_0^\infty \left(g_l^-(r)\right)^2 r^2\,\mathrm{d}r \tag{A.13}$$

$$F_+ = \int_0^\infty \left(f_l^+(r)\right)^2 r^2\,\mathrm{d}r \tag{A.14}$$

$$F_- = \int_0^\infty \left(f_l^-(r)\right)^2 r^2\,\mathrm{d}r \tag{A.15}$$

$$G_{+-} = \int_0^\infty g_l^+(r)g_l^-(r)r^2\,\mathrm{d}r \tag{A.16}$$

$$F_{+-} = \int_0^\infty f_{l+2}^+(r)f_l^-(r)r^2\,\mathrm{d}r \tag{A.17}$$

$$F_{-+} = \int_0^\infty f_{l-2}^+(r) f_l^-(r) r^2 \, \mathrm{d}r \tag{A.18}$$

$$F'_{-+} = \int_0^\infty f_l^+(r) f_{l+2}^-(r) r^2 \, \mathrm{d}r. \tag{A.19}$$

Apart from the case of G_+, G_-, F_+, F_- for $l = n - 1$, which are relatively easily obtained analytically, all other radial integrals have been calculated numerically (using quadruple precision).

The autocorrelation function can be calculated from (A.1) in a straightforward way:

$$\begin{aligned}\langle \Psi_r(0)|\Psi_r(t)\rangle = \sum_l \Bigg\{ & \exp\left(-\mathrm{i}E_l^+ t\right) \left[\sum_m w_{l,m}^2 \left(a^2 \frac{l+1+m}{2l+1} + b^2 \frac{l+1-m}{2l+1} \right) \right] \\ & + \exp\left(-\mathrm{i}E_l^- t\right) \left[\sum_m w_{l,m}^2 \left(a^2 \frac{l-m}{2l+1} + b^2 \frac{l+m}{2l+1} \right) \right] \Bigg\}\end{aligned} \tag{A.20}$$

Appendix B

Let us use the following notation:

$$k = j + 1/2 \qquad \mathcal{E}_k = \frac{E_{nlj}}{m_0 c^2} \qquad x = (Z\alpha)^2. \tag{B.1}$$

The exact eigenenergies $\mathcal{E}_k$ (in units of m_0c^2) are given by

$$\mathcal{E}_k = \left[1 + \frac{x^2}{(n - k + \sqrt{k^2 - x^2})^2} \right]^{-1/2}. \tag{B.2}$$

Expanding this expression in Taylor series with respect to x, one obtains

$$\mathcal{E}_k = 1 - \frac{x^2}{2n^2} - \frac{x^4}{4n^3}\left(\frac{2}{k} - \frac{3}{2n}\right) - \frac{x^6}{4n^3}\left(\frac{1}{2k^3} + \frac{3}{2nk^2} - \frac{3}{n^2k} + \frac{5}{4n^3}\right) + [O(x)]^8. \tag{B.3}$$

In equation (7) only the lowest term depending on k in x^4, i.e. $\delta_4\mathcal{E}_k = -\frac{x^4}{4n^3}\frac{2}{k}$, has been included. The higher order term $\delta_6\mathcal{E}_k$ contributes very little, because the ratio $\delta_6\mathcal{E}_k/\delta_4\mathcal{E}_k = x^2\left(\frac{1}{k^2} + \frac{3}{4nk} - \frac{3}{2n^2} + \frac{5k}{8n^3}\right)$ reaches the maximum value of about 0.0005 for $\epsilon = 0.4$ and $Z = 92$ and stays much smaller for lower Z. Then the time evolution for not too long period is mainly determined by the lowest order contribution (7).

The precession time is determined by the derivative

$$\left.\frac{\partial \mathcal{E}_k}{\partial k}\right|_{k=l_{av}} = \frac{x^4}{2n^3k^2}\left[1 + \frac{3x^2}{2}\left(\frac{1}{2k^2} + \frac{1}{nk} - \frac{1}{2n^2}\right)\right]. \tag{B.4}$$

Again in equations (8) and (9) only terms of the order of x^4 have been used. The x^6-order term contributes at most about 0.000 22 of the x^4-order term for $\epsilon = 0.4$ and $Z = 92$. Therefore, we conclude that the x^6-order term can be safely neglected in estimation of the precession time T_p.

References

[1] For an introduction and a list of references, see Schleich W P 2001 *Quantum Optics in Phase Space* (Berlin: Viley-VCH)

[2] Bosanac S D 1993 *J. Phys. A: Math. Gen.* **25** 5523

[3] Kylstra N J, Ermolaev A M and Joachain C J 1997 *J. Phys. B: At. Mol. Opt. Phys.* **30** L449

[4] Rathe U W, Keitel C H, Protopapas M and Knight P L 1997 *J. Phys. B: At. Mol. Opt. Phys.* **30** L531
[5] Rutherford G H and Grobe R 1998 *J. Phys. A: Math. Gen.* **31** 9931
[6] Su Q, Smetanko B A and Grobe R 1998 *Laser Phys.* **8** 93
[7] Braun J W, Su Q and Grobe R 1999 *Phys. Rev.* A **59** 604
[8] Wagner R E, Peverly P J, Su Q and Grobe R 1999 *Phys. Rev.* A **61** 035402
[9] Krekora P, Wagner R E, Su Q and Grobe R 2001 *Phys. Rev.* A **63** 025404
[10] Krekora P, Su Q and Grobe R 2001 *J. Phys. B: At. Mol. Opt. Phys.* **34** 2795
[11] Nilsen H M, Masden L B and Hansen J P 2001 *J. Phys. B: At. Mol. Opt. Phys.* **34** L39
[12] Arvieu R, Rozmej P and Turek M 2000 *Phys. Rev.* A **62** 022514
[13] Arvieu R and Rozmej P 1994 *Phys. Rev.* A **50** 4376
Arvieu R and Rozmej P 1996 *J. Phys. B: At. Mol. Opt. Phys.* **29** 1339
[14] Averbukh I S and Perelman N F 1989 *Phys. Lett.* A **139** 449
Averbukh I S and Perelman N F 1989 *Sov. Phys.–JETP* **69** 464
[15] Rozmej P, Arvieu R, Averbukh I S and Turek M 2001 *ECAMP VII, 7th European Conf. Atomic and Molecular Physics (Berlin, 2–6 April 2001) Europhys. Conference Abstr.* **25B** 99
[16] Gay J C, Delande D and Bommier A 1989 *Phys. Rev.* A **39** 6587
[17] Crawford M C 2001 *Am. J. Phys.* **69** 1182
[18] Chang E C 1985 *Phys. Rev.* A **31** 495
[19] Sommerfeld A 1921 *Atombau und Spektrallinien* (Braunschweig: Fievag)
[20] Rozmej P and Arvieu R 1999 *J. Phys. A: Math. Gen.* **32** 5637